Anup Karak, Dipankar Kundu and Somenath Sarkar*

Simplified Loss Estimation of Splice to Photonic Crystal Fiber using New Model

DOI 10.1515/joc-2015-0043
Received May 1, 2015; accepted September 23, 2015

Abstract: For a range of fiber parameters and wavelengths, the splice losses between photonic crystal fiber and a single mode fiber are calculated using our simplified and effective model of photonic crystal fiber following a recently developed elaborate method. Again, since the transverse offset and angular mismatch are the serious factors which contribute crucially to splice losses between two optical fibers, these losses between the same couple of fibers are also studied, using our formulation. The concerned results are seen to match fairly excellently with rigorous ones and consistently in comparison with earlier empirical results. Moreover, our formulation can be developed from theoretical framework over entire optogeometrical parameters of photonic crystal fiber within single mode region instead of using deeply involved full vectorial methods. This user-friendly simple approach of computing splice loss should find wide use by experimentalists and system users.

Keywords: photonic crystal fiber, spot size, splice loss, transverse offset, fundamental space-filling mode

PACS® (2010). 81.Bm, 42.81.Cn, 42.81.Dp, 42.81.Qb

1 Introduction

Study of photonic crystal fibers (PCF) and their propagation characteristics like dispersion, splice loss, are drawing enormous attentions. These fibers consist of a pure silica core surrounded by a periodic microstructure of silica and air-holes along the entire length [1]. Importance of these fibers lies in their various significant and unique characteristics [2, 3], such as endlessly single mode operation, large or ultra-small mode field diameters (MFDs) and hence effective areas, highly tailorable group velocity dispersion, and high nonlinearity [1–3], which are greatly useful in various optical fiber communication applications. However, the structural complexity, absence of rotational symmetry, and high index difference in PCFs make them much more complex to analyze this class of fibers theoretically or analytically. Several numerical methods such as effective index method (EIM) [2], finite-difference method [4], finite-element method (FEM) [5], multipole method [6], and step index fiber approximation (SIFA) [7] have been developed to predict various propagation characteristics of PCFs. But, all these numerical methods are very much deeply involved and one cannot easily develop them from the first principles or can appreciate them pedagogically.

Therefore, one can compute these characteristics easily with tolerable accuracy and without intricate computations if one has a simple and general method to obtain the effective cladding index of a PCF and, thereby, PCF characteristics. In fact, very recently, a simple, complete, and versatile method has been proposed to predict the effective cladding index of a PCF [8]. Once it is known for particular fiber parameters corresponding to the wavelength of practical interest, one can analog a PCF to a single mode conventional step index fiber (CSF) and predict propagation characteristics of PCF, more easily, in comparison to the available deeply involved numerical methods. The applicability of this method is also shown in respect of simple computations of waveguide dispersion, beam divergence, and mode field diameter and the fairly excellent match of the computed results of these quantities with available data.

However, splicing of a PCF with another PCF or one CSF, an important propagation characteristics, demands whether this elegant formalism is valid equally well in case of splice-loss calculation. In this context, it may be relevant to mention that numerous experiments and applications need PCFs to be spliced with CSF as well as PCFs with low losses [9]. The splice losses are mainly due to fundamental mode mismatch, as well as for transverse, angular, and longitudinal misalignment. So, minimization of the splice losses between PCF and CSF and between two PCFs is a matter of great concern, in practice.

***Corresponding author: Somenath Sarkar,** Department of Electronic Science, University of Calcutta, Kolkata 700009, India; Centre for Research in Nanoscience and Nanotechnology, University of Calcutta, Kolkata 700098, India
Anup Karak, Department of Electronic Science, University of Calcutta, Kolkata 700009, India; Centre for Research in Nanoscience and Nanotechnology, University of Calcutta, Kolkata 700098, India
Dipankar Kundu, Department of Electronic Science, University of Calcutta, Kolkata 700009, India; Centre for Research in Nanoscience and Nanotechnology, University of Calcutta, Kolkata 700098, India; Department of Electronics and Communication Engineering, St. Thomas' College of Engineering and Technology, Kolkata 700023, India

If appropriate structure parameters of PCFs based on theoretical or simulative analysis of splice loss are designed, splice loss can be minimized to a great extent.

In the recent past, attention is focused to compute the splice losses of PCF and CSF and various numerical techniques [9–12] have been used to estimate them between a PCF and a CSF and also between two identical PCFs. These techniques are complex in nature. Furthermore, it is essential to have adequate knowledge about the splice losses with respect to different parameters, like air-filling factor or relative air-hole size, hole-pitch of PCFs, so that the splice losses can be minimized by tailoring those PCF parameters [11]. So, as stated above, the development of an easier approach to estimate splice losses between PCF and CSF and also between two PCFs deserves attention as a simpler alternative. This approach should take into account not only all these factors without requirement of much effort and computational time but also should predict such loss in tolerably consistent manner through easy computations by experimentalists.

In this paper, we propose to apply a novel and simplified approach, as stated above, to estimate and predict the splice loss of PCF with a CSF, for the first time, for a range of known fiber parameters and wavelengths of the light. This approach involves evaluation of the effective cladding index of the PCF first, as explained in next section with brief detailing in Appendix, and then the effective normalized frequency or V-parameter and the spot size of the PCF. Also, our method needs computation in less number of relevant coefficients in comparison to the earlier one [8] for fixed wavelength of practical interest. Based on our formalism, we compute the splice losses of PCF and CSF interconnect from the available spot sizes of the PCF and CSF. In addition, we have also used the approach to compute splice loss of the PCF with CSF in presence of transverse offset and angular or tilt mismatch. We also show that our transverse offset splice-loss results are matching reliably with the available results. Further, a comparative study of the splice loss between the PCF and CSF obtained by our EIM, FEM, and SIFA method is carried out in this investigation.

2 Theory and analysis

2.1 Preview and formalism for spot size

We consider an all-silica PCF with triangular lattice of uniform air-holes of diameter d, along the entire length of the fiber, as in Figure 1. The holes are placed, symmetrically, around a central defect, made up of silica, acting as the fiber core. The air-hole matrix with lattice-constant or hole-pitch Λ is considered to act as the cladding of the PCF. The structure remains unchanged in the longitudinal direction. Since the core-index n_{CO} is greater than the effective cladding index n_{FSM}, the fiber can guide light by the process of modified total internal reflection like a CSF for longer wavelengths and by photonic bandgap mechanism for shorter wavelengths.

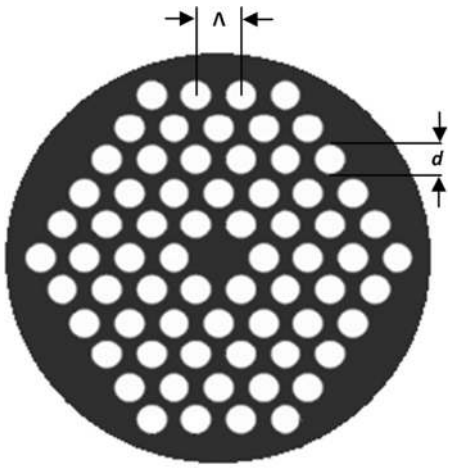

Figure 1: Index guided photonic crystal fiber cross-section.

The propagation constants β of the guided modes through the core of the PCF lie within upper and lower limits as follows [2]:

$$kn_{CO} > \beta > \beta_{FSM} \tag{1}$$

where $k = 2\pi/\lambda$, λ being the operating wavelength and n_{CO} is the refractive index of silica, the core material. Here, β_{FSM} is the propagation constant of the fundamental space-filling mode (FSM), the fundamental mode in the infinite photonic crystal cladding without any core or defect. This β_{FSM} is the maximum value of β in the cladding region of the said PCF.

Further, the effective cladding index or the index corresponding to the FSM is [2]:

$$n_{FSM} = \frac{\beta_{FSM}}{k} \tag{2}$$

The procedure to obtain the value of n_{FSM} for given fiber parameters and wavelength of light using [8] is elucidated in the Appendix section.

In Tables 1 and 2, all the values of the concerned coefficients found from least square fitting are presented in tabular form for the wavelengths $\lambda = 1.55$ μm and $\lambda = 1.31$ μm, respectively. These concerned coefficients are used to compute the n_{FSM} values of the PCF for

Table 1: Values of all coefficients for formulation of fundamental space-filling mode n_{FSM} at wavelength $\lambda = 1.55$ μm.

			$\lambda = 1.55$ μm
	$i = 0$	$i = 1$	$i = 2$
A_i	1.433434	0.001758	0.000007
B_i	0.061986	−0.006817	0.000036
C_i	−0.424058	0.115440	−0.009167

Table 2: Values of all coefficients for formulation of fundamental space-filling mode n_{FSM} at wavelength $\lambda = 1.31$ μm.

			$\lambda = 1.31$ μm
	$i = 0$	$i = 1$	$i = 2$
A_i	1.430536	0.003725	−0.000206
B_i	0.069106	−0.012302	0.000623
C_i	−0.377925	0.108040	−0.008822

various values of hole-pitch, Λ and relative hole sizes, d/Λ at a fixed wavelength of practical interest.

Now, the effective cladding index n_{FSM} can be used to find the effective V-parameter of the PCF, treating the PCF like a CSF with its core and cladding indices same as n_{CO} and the index n_{FSM}, respectively. This is known as effective index method. Our EIM [8] formulations are, extensively and elaborately, developed on the basis of scalar framework [1, 2]. Now, the effective Vvalue, V_{eff} of the PCF is given by

$$V_{eff} = \frac{2\pi}{\lambda} a_{eff} \left[n_{CO}^2 - n_{FSM}^2 \right]^{1/2} \tag{3}$$

where λ is the operating wavelength, n_{CO} is the core index, and a_{eff} is the effective core radius which is assumed [7] to be $\Lambda/\sqrt{3}$.

Then, the modal spot size w_{eff}, half of the MFD is obtained, using Marcuse formula [13, 14], given as:

$$\frac{w_{eff}}{a_{eff}} = 0.65 + \frac{1.619}{V_{eff}^{3/2}} + \frac{2.879}{V_{eff}^{6}} \tag{4}$$

The spot size of the PCF (w_{PCF}) is obtained using eq. (4), where V_{eff} is effective V-parameter, calculated from eq. (3). The spot size of single mode fiber (SMF), w_{SMF}, is also obtained by using Marcuse formula, where a_{eff} and V_{eff} are replaced by those of SMF in eq. (4) [13, 14].

2.2 Formulation for splice-loss calculation

According to Gaussian beam propagation formalism, the maximum power coupling between PCF and an SMF, for a perfectly aligned joint is given in terms of the above modal spot sizes, as [13, 14]:

$$\eta = \left(\frac{2 w_{PCF} w_{SMF}}{w_{SMF}^2 + w_{PCF}^2} \right)^2 \tag{5}$$

where w_{SMF} and w_{PCF} are the spot sizes of the SMF and PCF, respectively.

Therefore, the splice loss between PCF and an SMF in absence of any misalignments is obtained as

$$\alpha = -20 \log \left[\left(\frac{2 w_{PCF} w_{SMF}}{w_{SMF}^2 + w_{PCF}^2} \right) \right] \tag{6}$$

Again the power coupling between PCF and an SMF in presence of transverse misalignment between core centers of PCF and SMF is given by [13, 14]

$$\eta_T = \left(\frac{2 w_{PCF} w_{SMF}}{w_{SMF}^2 + w_{PCF}^2} \right)^2 . \exp \left(\frac{-2u^2}{w_{SMF}^2 + w_{PCF}^2} \right) \tag{7}$$

where u is the transverse offset.

Therefore, the splice loss between PCF and an SMF in presence of transverse misalignment can be written as

$$\alpha_T = -20 \log \left(\frac{2 w_{PCF} w_{SMF}}{w_{SMF}^2 + w_{PCF}^2} \right) + 4.34 \left(\frac{2u^2}{w_{SMF}^2 + w_{PCF}^2} \right) \tag{8}$$

Further, the power coupling between PCF and an SMF in presence of angular or tilt misalignment between core centers of PCF and SMF is given by [13, 14]

$$\eta_\theta = \left(\frac{2 w_{PCF} w_{SMF}}{w_{SMF}^2 + w_{PCF}^2} \right)^2 . \exp \left(\frac{(k_0 \theta \, w_{SMF} w_{PCF})^2}{2 \left(w_{SMF}^2 + w_{PCF}^2 \right)} \right) \tag{9}$$

where θ is the tilt offset.

Therefore, the splice loss between the PCF and SMF in presence of angular or tilt misalignment can be written as

$$\alpha_\theta = -20 \log \left(\frac{2 w_{PCF} w_{SMF}}{w_{SMF}^2 + w_{PCF}^2} \right) + 4.34 \left(\frac{(k_0 \theta \, w_{SMF} w_{PCF})^2}{2 \left(w_{SMF}^2 + w_{PCF}^2 \right)} \right) \tag{10}$$

when the two fibers are properly aligned, the transverse and angular offset is zero, the eqs (7) and (9) reduce to eq. (5) and eqs (8) and (10) reduce to eq. (6) and therefore the splice loss will be the minimum. Further, the splice loss starts to increase with increasing values of u and θ.

3 Results and discussion

In this section, we compute the splice loss of PCF with a CSF for different PCF parameters and wavelengths,

mentioned below, whereas for CSF, we take the SMF-28 type of CSF with core diameter 8.3 μm and core and cladding refractive indices as 1.5362 and 1.5306 respectively, as stated in preceding works [13].

3.1 The splice loss between PCF and SMF with variation of hole-pitch

We now compute the splice losses between the PCF and SMF-28 following eq. (6) with the variation of hole-pitch Λ for various relative hole sizes, d/Λ, values of 0.45 and 0.40, in decreasing order at an wavelength of λ = 1.55 μm. Further, in our calculation, we estimate the splice losses between PCF and SMF-28 in the endlessly single mode region of the PCF, since our EIM is taken in this region. We consider these two values of d/Λ as typical example [7, 10]. Here, we show our results of splice loss with variation of Λ in Figure 2(a) and 2(b) by solid curves. For comparison, we have considered $a_{\text{eff}} = \Lambda/\sqrt{3}$ for PCF in consistence with earlier work [7, 8]. Then we also compare splice losses computed by our EIM with those available in literature based on the vector FEM [10] shown by dotted curves and SIFA [7] shown by dash-dotted curves. On the basis of our EIM, we also see that, when the fibers are properly aligned, the splice loss is decreasing with increasing hole-pitch Λ for different relative hole sizes d/Λ. From the figures, it is seen that, obtained results are matching reliably with rigorously available results. However, we see that, our EIM, consistently but predictably, underestimates the splice loss whereas SIFA results, although mostly in between FEM and ours appear to be inconsistent. Accepting the rigorous FEM results as standard, SIFA over estimates FEM results at lower Λ and gradually underestimates the later at higher Λ. But, so far as the consistency in trend is concerned, our EIM stands as a reliable candidate in comparison to SIFA. However, we should emphasize in this context, that SIFA calculates the effective cladding index n_{FSM} by applying full vectorial finite element calculation only to central unit cell, consisting of central and surrounding hexagonal air-holes, taken as cladding [7]. The use of such FEM is deeply involved whereas our formulations are not only presented as ready reference but also can be derived right from fundamental principle. Thus, in our EIM, one can easily and pedagogically derive the n_{FSM} directly from known equation in the scalar framework [1, 2, 8] explained in Appendix. Thus overview of the results obtained for our EIM, FEM and SIFA methods favors our EIM method only for its simplicity but at the expanse of accuracy. However, in order to utilize the simplicity, we feel that simple correction scheme can be proposed to scale the raw results of splice-loss estimation using our EIM by suitable fitting to the true loss.

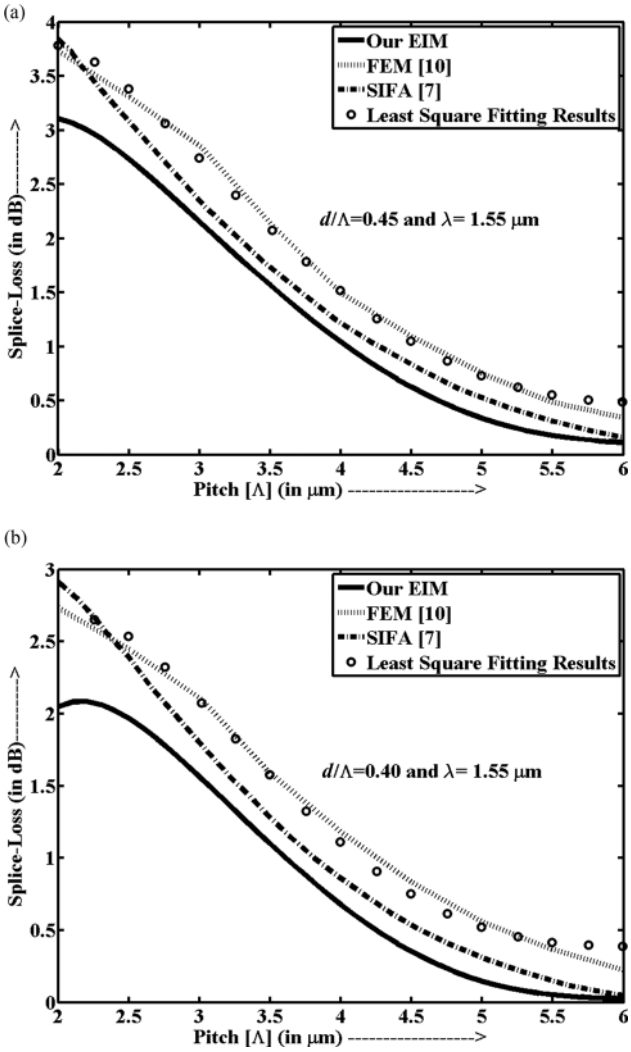

Figure 2: (a) Splice-losses with variation of hole pitch Λ at wavelength $\lambda = 1.55\,\mu m$ and relative hole size $d/\Lambda = 0.45$. (b) Splice-losses with variation of hole pitch Λ at wavelength $\lambda = 155\,\mu m$ and relative hole size $d/\Lambda = 0.40$.

In this context, a nonlinear polynomial fit of FEM splice loss (α_{FEM}) results in terms of our EIM splice loss (α_{EIM}) results is carried out as $\alpha_{\text{FEM}} = a + b\alpha_{\text{EIM}}$. We take α_{FEM} as our true loss. Here, we take a set of Λ values for d/Λ = 0.45 and 0.40 at wavelength λ = 1.55 μm and calculate the α_{EIM} and α_{FEM}. These calculated splice-loss values are then used in the above fitting equation and the values of fitting coefficients are obtained as a = 0.358842 and b = 1.104656. The splice-loss results using the fitting coefficients are also shown by circles in the Figure 2(a) and 2(b), where it is clearly evident that, the computed results using these fitting coefficients are almost excellently matching with the true losses.

3.2 The splice loss between PCF and SMF with the variation of transverse offset

Now, we estimate the transverse splice losses between the PCF and SMF-28 following eq. (8) with variations of transverse offset length (u) at hole-pitch $\Lambda = 6$ μm and $d/\Lambda = 0.458$ [12] for two different wavelengths $\lambda = 1.55$ μm and 1.31 μm. Then, we have plotted the variation of splice loss with offset length in Figure 3(a) and 3(b) for the same two wavelengths $\lambda = 1.55$ μm and 1.31 μm, respectively, and our results are shown by solid line, whereas dotted curves are representing FEM and dash dots, the MFD results [12]. The MFD results are based on formulation of mode field diameter, developed from involved numerical integration and finite element calculations of mode fields and, hence, not easily accessible from first principles.

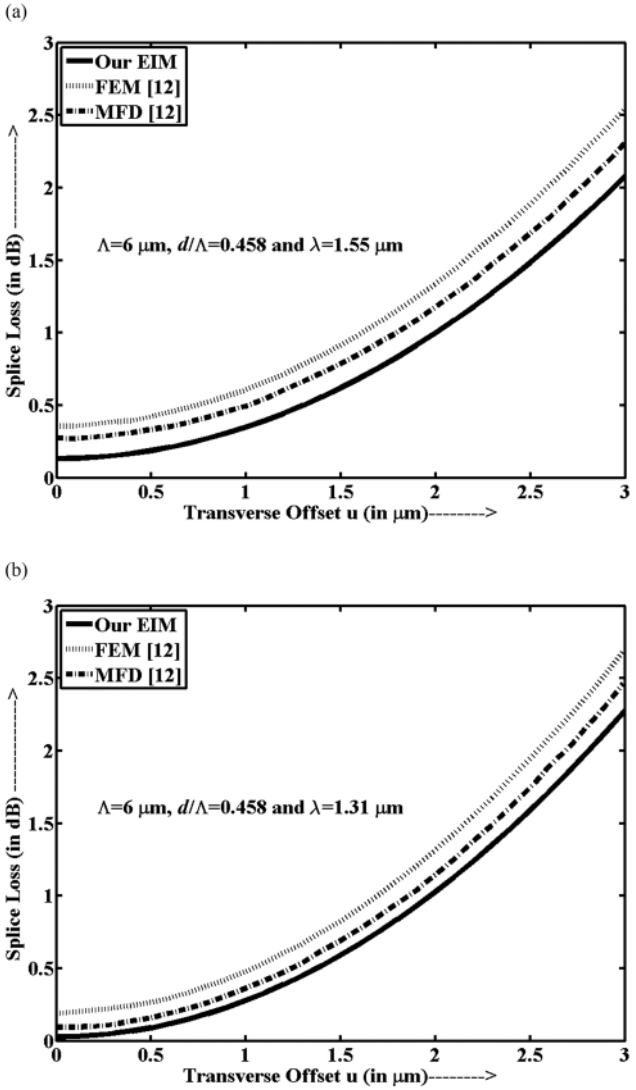

Figure 3: (a) Splice-loss between single mode fiber and photonic crystal fiber with variation of Transverse offset for wavelength $(\lambda) = 155\,\mu m$ relative hole size (d/Λ) =0.458 and hole Pitch $(\lambda) = 6\,\mu m$. (b) Splice Loss between single mode fiber and photonic crystal fiber with variation of Transverse offset for wavelength $(\lambda) = 1.31\,\mu m$ relative hole size (d/Λ) =0.458 and hole Pitch $(\Lambda) = 6\,\mu m$.

It may be noted that our EIM model is valid for $d/\Lambda \le 0.45$ in endlessly single-moded region. But, here we consider the cases for $d/\Lambda = 0.458$, falling just beyond the borderline of this region. We have to consider this case for the sake of comparison with the available results [12]. Even then, we see an impressive match with those obtained from FEM and MFD techniques, shown in Figure 3(a) and 3(b). Here, we have considered $a_{eff} = \Lambda/\sqrt{3}$ as in [7]. It is seen that, our computed splice loss in presence of transverse misalignment is increasing with the increase in transverse offset length for a particular wavelength, relative hole sizes d/Λ, and hole-pitch Λ following similar tends.

It may be relevant to mention that, in our transverse splice-loss calculation, we compute the spot size using well-known Marcuse formulation in eq. (4) which is simple and easy to understand and then we find the splice loss. On the other hand, MFD results of [12] are calculated on the basis of a different expression of PCF spot size, lacking in wide use as enjoyed by Marcuse relations. Moreover, whereas our spot size can be, directly, calculated right from scratch using our EIM model based on [2], it is difficult to deduce the MFD expressions of [12]. It may be relevant to point out that like the procedure of fitting in Section 3.1 in case of absence of misalignment, we can proceed similarly to propose a least square fitting procedure to scale the raw splice losses to true or FEM-based splice losses in Figure 3(a) and 3(b) in case of presence of transverse misalignment.

3.3 The splice loss between PCF and SMF with the variation of angular offset

Now, we estimate the angular splice losses between the PCF and SMF-28 following eq. (10) with variations of angular mismatch (θ) at hole-pitch $\Lambda = 6$ μm for $d/\Lambda = 0.45$ and 0.40. Then, we have plotted the variation of splice loss with angular mismatch in Figure 4(a) and 4(b) for the two wavelengths $\lambda = 1.55$ μm and 1.31 μm, respectively, and in the figures the solid line represents the $d/\Lambda = 0.45$ results, whereas dash-dotted curves are representing $d/\Lambda = 0.40$. Here also, we have considered $a_{eff} = \Lambda/\sqrt{3}$ as in [7]. It is seen that, our

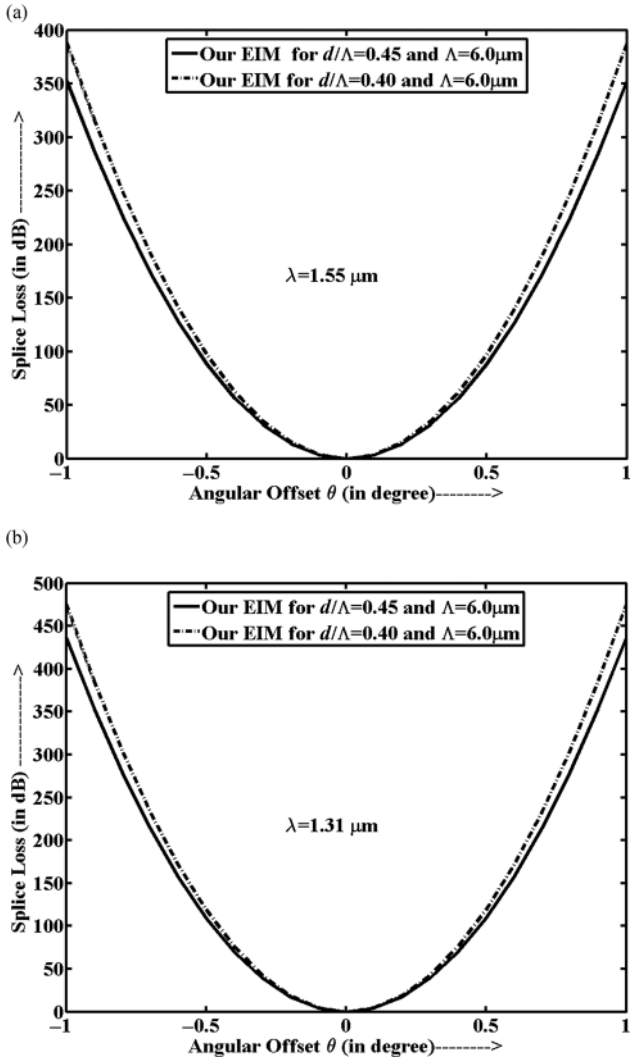

Figure 4: (a) Splice Loss between single mode fiber and photonic crystal fiber with variation of Angular offset for wavelength (λ) = 1.55 μm and hole Pitch (Λ) = 6 μm at relative hole size (d/Λ) =0.45 and 0.40. (b) Splice Loss between single mode fiber and photonic crystal fiber with variation of Angular offset for wavelength (λ) = 1.31 μm and hole Pitch (Λ) = 6 μm at relative hole size (d/Λ) =0.45 and 0.40.

computed splice loss in presence of angular misalignment is increasing with the increase in angular mismatch for a particular wavelength, relative hole sizes d/Λ, and hole-pitch Λ. Our calculations related to splice losses for tilt are expected to generate interest in system designers to use our results.

To summarize, we have justified the simplicity and reliability of our method of calculation of splice loss based on our simplified EIM which can be developed from first principle. Further, we believe that the method would impress the system users to estimate, readily, such losses without much computations.

4 Conclusion

We have calculated the splice losses between the PCF and an SMF, using our simple approach based on a very recently developed complete formulation for a wide range of fiber parameters and wavelengths. Our approach is made more simple since we take a fixed wavelength for practical application and thereby present less number of relevant coefficient required for effective cladding index calculation. Also the splice losses between the PCF and an SMF in presence of transverse offset and angular mismatch are studied using our simple formulation. It is clearly evident that the transverse offset splice-loss results obtained using this approach are matching fairly excellently with available results. This stands to justify validity the proposed computational schemes as reliable alternative to compute splice loss by our EIM model for easy estimation of propagation characteristics of practical interest and wide use by system users. Further, we proposed a least square fitting formulation to fit our simple but approximate loss values to true splice-loss values. This formulation should find wide attention of the system designers as ready reference.

Acknowledgment: The authors are grateful to the Centre for Research in Nanoscience and Nanotechnology (CRNN), University of Calcutta for infrastructural support. The first author gratefully acknowledges the financial support for award of senior research fellowship of UGC by CRNN, CU. The authors gratefully acknowledge anonymous reviewer for constructive suggestions.

Appendix

The normalized parameters v and u for the infinite cladding region of the chosen PCF are given by [1]:

$$v = k\Lambda\left(n_{CO}^2 - 1\right)^{1/2} \tag{11}$$

and

$$u = k\Lambda\left(n_{CO}^2 - \frac{\beta^2}{k^2}\right)^{1/2} \tag{12}$$

with

$$u^2 + w^2 = v^2 \tag{13}$$

To obtain the n_{FSM}, a basic air-hole at the center of a hexagonal unit cell is approximated to a circle in a

regular photonic crystal [2]. Then, from relevant boundary conditions for the fields and their derivatives in terms of appropriate special functions, corresponding to a fixed value of v, obtained from eq. (11) for fixed λ and Λ-values, the value of concerned u is computed from the following equation [1]:

$$\begin{aligned} &wI_1(a_n w)[J_1(bu)Y_0(a_n u) - J_0(a_n u)Y_1(bu)] \\ &+ uI_0(a_n w)[J_1(bu)Y_1(a_n u) - J_1(a_n u)Y_1(bu)] = 0 \end{aligned} \tag{14}$$

where $a_n = \frac{d}{2\Lambda}$, $b = \left(\frac{\sqrt{3}}{2\pi}\right)^{1/2}$.

Using eq. (14), Russell has provided a polynomial fit to u, only for $d/\Lambda = 0.4$ and $n_{CO} = 1.444$. However, for all d/Λ values of practical interest in the endlessly single mode region of a PCF, where d/Λ is less than or equal to 0.45, one should have a more general equation for wide applications.

Then the roots, that is, the u-values are obtained from eq. (14), for different d/Λ values at a particular λ, taking $n_{CO} = 1.45$. The values of n_{FSM} are determined by replacing β/k in eq. (12) with n_{FSM} and this has enabled us to propose a modified simpler formulation of [8] as follows:

$$n_{FSM} = A + B\left(\frac{d}{\Lambda}\right) + C\left(\frac{d}{\Lambda}\right)^2 \tag{15}$$

where A, B and C are three different optimization parameters, dependent on both the relative hole-diameter or hole-size d/Λ and the hole-pitch Λ. Here we take up to quadratic term in eq. (15), which is providing tolerable accuracy at a less cumbersome computation.

Since, the operating wavelengths used in optical communication system are $\lambda = 1.55$ μm and 1.31 μm, we only find the coefficients for these two wavelengths for different possible hole-size and hole-pitch. Such modification in the fitting is advantageous in the manner that, it will help us to reduce computation time, since only 9 coefficients are required to compute instead of 27 coefficients [8].

Now, for each value of Λ with the variations of d/Λ, we determine the n_{FSM} values consequent to u values obtained from eq. (14). Applying least square fitting of n_{FSM} in terms of d/Λ to eq. (15) for a particular Λ, we then estimate the values of A, B and C. The various values of A, B and C are then simulated for different Λ in the endlessly single mode region of the PCF, resulting in the empirical relations of A, B and C in eq. (15), in terms of Λ, as given in the following:

$$A = A_0 + A_1\Lambda + A_2\Lambda^2 \tag{16}$$

$$B = B_0 + B_1\Lambda + B_2\Lambda^2 \tag{17}$$

$$C = C_0 + C_1\Lambda + C_2\Lambda^2 \tag{18}$$

where A_i, B_i and C_i ($i = 0$, 1, and 2) are the optimization parameters for A, B and C respectively. These A, B and C in eq. (15) are same as those in eqs (16)–(18). Computing A, B and C from eqs (16)–(18), one can find n_{FSM}-s directly for any Λ and d/Λ value at any particular λ in the endlessly single mode region of the PCFs, using eq. (15).

References

1. Russell PS. Photonic-crystal fibers. IEEE J Lightwave Tech 2006;24:4729–49.
2. Birks TA, Knight JC, Russell PS. Endlessly single-mode photonic crystal fiber. Opt Lett 1997;22:961–3.
3. Park KN, Lee KS. Improved effective-index method for analysis of photonic crystal fibers. Opt Lett 2005;30:958–60.
4. He YJ, Shi FG. Finite-difference imaginary-distance beam propagation method for modeling of the fundamental mode of photonic crystal fibers. Opt Commun 2003;225: 151–6.
5. Brechet F, Mercou J, Pagnoux D, Roy P. Complete analysis of the characteristics of propagation into photonic crystal fibers by the finite element method. Opt Fiber Technol 2000;6: 181–91.
6. White TP, McPhedran RC, Botten LC, Smith GH, de. Sterke CM. Calculations of air-guided modes in photonic crystal fibers using the multipole method. Opt Express 2001;9: 721–32.
7. Koshiba M, Saitoh K. Applicability of classical optical fiber theories to holy fibers. Opt Lett 1741;29:1739–41.
8. Kundu D, Sarkar S. Prediction of Propagation characteristics of photonic crystal fibers by a simpler, more complete and versatile formulation of their effective cladding indices. Opt Eng 2014;53:056111.
9. Xu Z, Duan K, Liu Z, Wang Y, Zhao W. Numerical analyses of splice losses of photonic crystal fibers. Opt Commun 2009;282:4527–31.
10. Hoo YL, Jin W, Ju J, Ho HL. Loss analysis of single-mode fiber/photonic-crystal fiber splice. Microwave Opt Technol Lett 2004;40:378–80.
11. Lizier JT, Town GE. Splice losses in holey optical fibres. IEEE Photon Technol Lett 2001;13:466–7.
12. Ju J, Jin W, Hoo YL, Demokan MS. A simple method for estimating the splice loss of photonic-crystal fiber/single-mode fiber. Microwave Opt Technol Lett 2004;42:171–3.
13. Marcuse D. Loss analysis of single-mode fiber splices. J Bell Syst Tech 1977;56:703–18.
14. Ghatak AK, Thyagarajan K. Introduction to fiber optics. UK: Cambridge University Press, 1998.